RSC Advances

ROYAL SOCIETY OF CHEMISTRY

www.rsc.org/advances

Emulsion Polymerization for Fabrication of Poly (o-phenylenediamine) @ Multi-walled Carbon Nanotubes nanocomposite: Characterization and Its Application to the Corrosion Protection of 316L SS

Ehsan Nazarzadeh Zare[a], Moslem Mansour Lakouraj[a*], Shahram Ghasemi[b], Elham Moosavi[a]

[a] Department of Organic-Polymer Chemistry, Faculty of Chemistry, University of Mazandaran, Babolsar, Iran

[b] Nanochemistry Research Laboratory, Faculty of Chemistry, University of Mazandaran, Babolsar, Iran

E-mail: lakouraj@umz.ac.ir; Tel-fax: +981125342350; postal code: 47416

Abstract

Recently, the corrosion of metals is an important academic and industrial concern which has received a significant attention. Poly (o-phenylenediamine) (PoPDA) based nanocomposites with unfunctionalized multi-walled carbon nanotubes (MWCNTs) and functionalized multi-walled carbon nanotubes (FMWCNTs) were prepared through emulsion polymerization using sodium dodecyl sulfate (SDS) as an emulsifier and ammonium persulfate (APS) as an oxidant. Fourier transform infrared (FT-IR) spectra were confirmed the construction of nanocomposites. The morphology of synthesized nanocomposites was characterized by scanning electron microscopy (SEM). X-ray diffraction (XRD) patterns of the nanocomposites indicated more crystalline nature than that of the bare PoPDA. Thermal stability of nanocomposites was improved relative to bare PoPDA. The corrosion protection performance of the coatings containing PoPDA@MWCNTs, PoPDA@FMWCNTs and PoPDA on steel was evaluated using potentiodynamic polarization, electrochemical impedance spectroscopic (EIS) and open circuit potential (OCP) measurements in 3.5 % NaCl solution. The obtained results of potentiodynamic polarization, EIS and OCP showed the PoPDA@MWCNTs nanocomposite coated steel had excellent corrosion inhibition behavior in saline solution.

Keywords: Emulsion polymerization, poly (o-phenylenediamine), multi-walled carbon nanotubes, steel, corrosion protection

Introduction

Polymer based nanocomposites have interested great research and development owing to their widespread applications in numerous fields such as, removal of heavy metal ions, sensors and anticorrosion coatings[1–3] . Specifically, the preparation of nanocomposites involving carbon nanotubes (CNTs) and conducting polymers (CPs) has been extensively studied in recent years due to the synergistic effects resulting from the combination of these materials[47].

The CPs based on aromatic diamines have been synthesized via polymerization of corresponding diamines monomers in the presence of an peroxy-initiator under acidic condition. They are displayed more novel multi functionality than PANI due to one pendent free amino group per repetitive unit on the polymer chains. In addition, they have shown good solubility in common organic solvents than PANI, but their conductivity is poor [8-10].

Among them, poly (o-phenylenediamine) (PoPDA) containing 2, 3-diaminophenazine or quinoraline repeating unit has gradually become an important member in the family of conductive polymers and it could be used in many fields[11,12]. However, PoPDA has poor physical properties. One method to improve of physical properties of the CPs is the use of inorganic nanoparticles in PANI-derivatives nanocomposites.

CNTs have gained considerable attention over the last decade due to their unique physical properties such as large surface area, good corrosion resistance, high temperature stability, and mechanical properties[13]. The formation of nanocomposite materials through the incorporation of CNTs into the polymer matrix (CNTs@polymer) is a valuable approach to enhance the mechanical properties, thermal stability, electrical conductivity, solvent resistance, and optical properties of the materials relative to individual components. For this purpose, a

number of methods have been developed to fabrication of CNTs @ polymer composites based on type of polymeric matrices[14,15].

One of the suitable methods for preparation of nanocomposites bearing polymer matrices is emulsion polymerization. Emulsion polymerization is the most commonly used method for the production of a wide range of polymers. This method allows particles to transfer into micelles through the emulsifier template and increase the molecular weight[10]. The CPs @ CNTs composites film have expected to act as an excellent coating materials for corrosion protection applications.

Recently, the corrosion of metals is an important academic and industrial concern which has received a significant attention. Many corrosion control methods use coatings and resistant layers that contain toxic and environmentally hazardous materials, especially chromium compounds. Hence, efforts should be made to develop pinhole-free coatings that satisfy the environmental concerns in order to avoid heavy metals. The CPs and CPs based nanocomposite are the promising options for protection of metals against corrosion. Recently, many researchers were reported the protection of CPs and CPs based nanocomposite against of corrosion.

For instance, Sathiyanarayanan et al. were prepared polyaniline/TiO_2 composite for protection of steel[16]. Kumar et al. investigated corrosion protection of PANI@FMWCNT nanocomposite [17]. Ionita et al. used of polypyrrole@carbon nanotube composites as an anti-corrosive coating[18]. Ganash studied anticorrosive properties of poly (o-phenylenediamine)@ZnO nanocomposites [19]. Olad et al. considered polypyrrole nanocomposites with organophilic and hydrophilic montmorillonite as corrosion protection on iron [3]. Lenz et al. investigated application of polypyrrole@TiO_2 composite films as corrosion protection [20]. Emamgholizadeh et al. investigated corrosion inhibition of steel by EP/PpPDA/SiO_2 nanocomposite [21].

The goal of this study is preparation of poly (o-phenylenediamine) based nanocomposites with functionalized and un-functionalized multi-walled carbon nanotubes via emulsion polymerization. Furrier transform infrared (FTIR), X-ray diffraction (XRD), thermal gravimetric analysis (TGA) and scanning electron microscopy (SEM) applied for characterization of the synthesized nanocomposites. Finally corrosion inhibition of synthesized nanocomposite against 316L stainless steel in 3.5% NaCl solution was investigated.

Experimental

Materials

Ortho-phenylenediamine (oPDA), ammonium persulfate (APS), sodium dodecyl sulfate (SDS) and all solvents were purchased from Merck Company (Germany) and were used without further purification. Multi-walled carbon nanotubes (MWCNTs) particles (diameter 20–50 nm, length 5–20 lm) were supplied from Sigma-Aldrich Company.

Characterization

Fourier transform infrared (FTIR) spectra were recorded on a Bruker Tensor 27 spectrometer (Bruker, Karlsrohe, Germany). X-ray diffraction (XRD, Shibuya-ku, Tokyo, Japan) patterns were obtained in the 2 theta range of 10–70° using a Rigaku D/Max-2550 powder diffractometer with a scanning rate of 5° min^{-1} at room temperature. Thermal gravimetric analysis (TGA) of prepared polymers and composites were determined using the LENSES STAPT-1000 calorimeter (Linseis STA PT1000, Selb, Germany) by scanning up to 700 °C with the heating rate of 10 °C/min. Scanning electron microscopy (SEM) was recorded on a Hitachi S4160 instrument (Tokyo, Japan). Potentiostat polarization and open-circuit potential were

recorded by Autolab 302 N (Netherlands). Also, electrochemical impedance spectroscopy was carried out by Palmsense (PS Trace software version 4.2.2, Netherlands).

Functionalization of multi-walled carbon nanotubes (FMWCNTs)

MWCNTs were functionalized according to our previous work [5]. MWCNTs (1g) were preserved in 200 mL oxidizing mixture of H_2SO_4/HNO_3 (3:1 v/v) (6 M) to prevent massive structural destruction of MWCNTs. Then mixture was dispersed by a sonication bath for 8 h at 50 °C. Then, the functionalized MWCNTs were neutralized to pH 7.0, centrifuged and washed with water/acetone (1:1) three times and separated by centrifuge. The filtered product was then dried under vacuum at 40 °C oven for 12 h.

Preparation of poly (o-phenylenediamine) based nanocomposites with un-functionalized and functionalized multi-walled carbon nanotubes

Poly(o-phenylenediamine) @ un-functionalized multi-walled carbon nanotubes (PoPDA@ MWCNTs) and poly (o-phenylenediamine) @ functionalized multi-walled carbon nanotubes (PoPDA@ FMWCNTs) nanocomposites were prepared by emulsion polymerization at room temperature as follows: In a typical experiment, 7.5 % (0.081 g) CNTs (optimum amount), 2.5 g (8.66 mmol) SDS, and 30 mL $CHCl_3$ were added into 30 mL of distilled water and the mixture was dispersed by an sonication bath at room temperature for about 2 h. Then, 30 mL of oPDA solution (1 g in 30 mL of HCl (1 M) was added to the above solution. The APS solution (1.5 g of APS in 20 mL deionized water) as an initiator was dropped into the reaction medium within 40 min and the reaction was carried out at room temperature for 24 h. Afterward, the mixture was poured into acetone to terminate the reaction. Finally, obtained precipitate filtered and washed with distilled water and methanol for several times and then was dried in

vacuum at 50 °C for 24 h. For comparative study, bare PoPDA was also synthesized via radical oxidation polymerization of oPDA in acidic medium according to our pervious report[10].

Corrosion tests

Tafel tests were carried out using a conventional three-electrode electrochemical cell with platinum wire as counter electrode, Ag/AgCl as a reference electrode, and the PoPDA, PoPDA@MWCNTs and PoPDA@FMWCNTs nanocomposites coated on 316L stainless steel (SS), and uncoated 316L SS samples as a working electrodes.

To prepare electrodes, firstly 2 g of polyvinyl butyral (PVB) (as adhesion agent) was dissolved in 20 mL of methanol and then 20 wt.% (0.5 g) of powder sample was added. The mixture solution was kept under sonication batch for 30 min to obtained a uniform dispersion of sample (PoPDA, PoPDA@MWCNTs and PoPDA@FMWCNTs) in the PVB solution. Steel electrode with a surface area of 0.07 cm^2 was then dip coated with the synthesized materials/PVB in methanol solution and dried at 60 °C temperature for 50 min. A NaCl 3.5% (w/w) electrolyte was used as corrosive environment.

Electrochemical impedance spectroscopy (EIS) measurements were done with frequencies ranging from 20 to10 KHz with the amplitude of the superimposed AC signal was 10 mV. Polarization curves for uncoated and polymer coated SS specimens were recorded under potentiodynamic conditions in the potential range of ± 250 mV with respect to OCP at a sweep rate of 2 mV s^{-1}.

Results and Discussion

Nowadays, the use of polymers and polymer matrix based nanocomposites for the inhibition of metals corrosion is one of the most applied approaches. Scheme 1 presents a typical

procedure for fabrication of PoPDA@FMWCNTs nanocomposites through emulsion polymerization technique and electrode construction pathway.

Scheme 1

FTIR analysis

FTIR spectra were used to characterize the functional groups of the synthesized PoPDA@MWCNTs and PoPDA@FMWCNTs nanocomposites, which were presented in Fig. 1.

To the best of our knowledge no significant functional groups were detected on the FTIR spectra of MWCNTs. Thus, the observed peaks at around 3325 and 1220 cm^{-1} are ascribed to the presence of hydroxyl groups of adsorbed water on the surface of MWCNTs, which could be appeared either from humidity bound to the MWCNTs or during the purification of raw material [22]. On the other hand, the FMWCNTs exhibit a characteristic peaks at 3356, 1680 and 1080 cm^{-1} can be attributed to the stretching vibrations of O–H, C=O of carboxylic acid and C-O, respectively[5]. Presence of these peaks suggests that oxidation of the MWCNTs have introduced COOH groups on the surface of MWCNTs. In the FTIR spectra of PoPDA, the peaks at 3380, 1630 and 1500 cm^{-1} can be attributed to N–H stretching vibration of the secondary amine group in the polymer chain, quoined and benzenoid stretching vibrations, respectively [12]. The FTIR spectra of the MWCNTs, FMWCNTs and PoPDA are presented in Fig. S1 in supplementary data.

The FTIR spectra of PoPDA@MWCNTs nanocomposite showed almost identical characteristic peaks at 3360, 1660, 1497, and 1210 cm^{-1}, respectively, which were in accordance with the previous reports composites with un-functionalized MWCNTs [23]. This approved that the PoPDA@MWCNTs nanocomposites had been successfully synthesized. In the FTIR spectra of PoPDA@FMWCNTs nanocomposite most of the FMWCNTs signals have been overlapped by

those of PoPDA. The characteristic peaks of PoPDA detected at 3390, 1630, and 1500 cm^{-1} were slightly shifted to lower wave numbers and became very weak. The reasonable response for this may be attributed to the formation of hydrogen bonding between the amino groups of the PoPDA and hydroxyl of the carboxylic groups in FMWCNTs.

Fig. 1

XRD diffraction

XRD diffraction (XRD) is a rapid analytical technique primarily used for phase identification of a crystalline material. In the XRD patterns of the MWCNTs and FMWCNTs three main peaks observed at 2θ = 25.9° and 41.02°, and 55.11° which designated their crystalline nature[24,25]. Meanwhile in XRD pattern of PoPDA, three broad characteristic peaks appeared at 2θ = 21°, 24° and 27° revealing that the local crystallinity may be caused by the periodicity perpendicular to the polymer chain[11]. The partial crystallinity may be resulted from the long range ordering of polymer chains in PoPD backbone[11]. The XRD patterns of the MWCNTs, FMWCNTs and PoPDA are presented in Fig. S2 in supplementary data.

The XRD patterns of PoPDA@MWCNTs and PoPDA@FMWCNTs nanocomposites exhibit two clear phases: the polymer phase and the MWCNTs phase, which has several sharp peaks. It specifies that the PoPDA@MWCNTs and PoPDA@FMWCNTs nanocomposites are higher crystalline than the bare PoPDA. In comparison to the PoPDA@MWCNTs and PoPDA@FMWCNTs nanocomposites, the crystalline structure of the PoPDA@FMWCNTs nanocomposite showed an improved relative to PoPDA@MWCNTs nanocomposite. This good crystalline nature probably appeared due to intramolecular interaction between carboxyl groups of FMWCNTs and amine groups of PoPDA.

Fig.2

SEM micrographs

Scanning electron microscopy (SEM) is extensively used in surface analysis of the synthesized materials. Fig. 3 demonstrates the SEM micrographs of PoPDA@MWCNTs and PoPDA@FMWCNTs nanocomposites.

As seen in Fig. S3a, it reveal that the PoPDA particles have irregular granules with a fairly different size distribution around 100–150 nm in average diameter. The MWCNTs morphology was exhibited boundless, twisted, with a smooth surface, and the diameter of each nanotube is about 20–50 nm (Fig. S3b). The SEM of FMWCNTs showed the extrication of the FMWCNTs, and slight reduction in the length of the nanotubes is observed after oxidation (Fig. S3c). The SEM images of the MWCNTs, FMWCNTs and PoPDA are presented in Fig. S3 in supplementary data.

As evident Fig.3a, indicates distribution of MWCNTs and disordered granular particles of PoPDA which represents absence of interaction between MWCNTs and PoPDA in the nanocomposite. In the SEM image of the PoPDA@FMWCNTs nanocomposite (Fig.3b), a tubular layer of coated PoPDA film is observed, and the diameter of the nanocomposite is increased by several tens of nanometers as compared with the FMWCNTs, depending on the PoPDA content. It can be attributed that the coating of PoPDA takes place only at the outer surface of the FMWCNTs. In fact, the formation of the PoPDA coated tubular nanocomposite is believed to arise from the strong interaction between the amine groups of PoPDA and carboxyl groups of FMWCNTs.

Fig.3

TGA analysis

Thermo gravimetric analysis (TGA) is a useful technique about the thermal stability of synthesized materials. Fig. 4 exhibited the TGA thermograms of PoPDA@MWCNTs and PoPDA@FMWCNTs nanocomposites.

As seen from TGA, thermogram of MWCNTs and FMWCNTs (Fig. S4), the COOH content in FMWCNTs is about 5.6 wt%, a reasonable value for acid treated MWCNTs [26]. TGA thermogram of PoPDA (Fig. S4) has two-step of thermal transition that lead to weight loss. The first thermal transition from 100 to 315 °C with a weight loss of ~11% correspond to the removal of, residual water, dopants and loss of low molecular weight oligomers[12]. The second transition which observed between 315 °C to 600 °C with a weight loss of ~45% can be attributed to the degradation of the backbone units of the PoPDA (benzenoid and quinoid units) [11]. The char yield at 800 °C is ~45%. The TGA thermograms of the MWCNTs, FMWCNTs and PoPDA are presented in Fig. S4 in supplementary data.

The comparison of the PoPDA, PoPDA@MWCNTs and of PoPDA@FMWCNTs nanocomposites, showed the improvement of the thermal stability of the nanocomposites relative to PoPDA, where residual weight at 800 °C for PoPDA@MWCNTs and of PoPDA@FMWCNTs nanocomposites is ~55 % and ~50 %, respectively.

Fig. 4

Potentiodynamic polarization studies

In this study polyvinyl butyral (PVB) was used as a binder for coating of synthesized material on steel electrode surface. The obtained results indicated that the PVB had no

anticorrosion activity against steel. To gain a better understanding the Tafel plots of uncoated and PVB coated steel in 3.5% w/w NaCl solution are given in Fig. S5 in Supplementary data.

Fig. 5 illustrates the Tafel plots for PoPDA, PoPDA@FMWCNTs, PoPDA@MWCNTs nanocomposites coated steel samples and uncoated steel in 3.5% w/w NaCl solution under potentiodynamic polarization conditions. The corrosion protection of the synthesized materials coated steel can be observed from the values of corrosion potential (E_{corr}), corrosion current (I_{corr}), and polarization resistances ($R_{p)}$ as listed in Table 1; generally, a higher E_{corr} and a lower I_{corr} indicate better corrosion protection. As seen from Tafel plot of the PoPDA@FMWCNTs nanocomposite coated steel, the I_{corr} of PoPDA@FMWCNTs nanocomposite was 222, which was higher than that of PoPDA@MWCNTs nanocomposite coated steel and lower than that of the PoPDA coated steel. Thus, it was found that the incorporation of FMWCNTs in PoPDA matrix improves the anticorrosive efficiency of PoPDA@FMWCNTs nanocomposite coating on steel sample. The anticorrosion activity of nanocomposites was more favorable at an optimum content of MWCNTs and FMWCNTs because adhesion strength of nanocomposite coating on steel decreases with increasing of MWCNTs content. Hence, in this study we carried out the anticorrosion activity experiments just for optimized nanocomposites. Furthermore, it is observed that, the E_{corr} of synthesized materials coated steel is shifted in the positive direction compared to that of uncoated steel. These positive shifts of -184 mV to -113 mV in E_{corr} indicate the protection of the steel surface by the synthesized material coatings where the best results obtained for PoPDA@MWCNTs coated steel with E_{corr} = -113. It is reasonable response that presence of π electrons in aromatic ring and quaternary nitrogen atom in PoPDA emeraldine salt and good conjugation in MWCNTs are important factors to effectively prevent steel against of corrosion.

On the other hand, the polarization resistances ($R_{p)}$ were calculated from the Tafel plots, giving to the Stearn-Geary equation [27]

$$R_p = \frac{b_a b_c}{2.303(b_a + b_c)I_{corr}} \qquad (1)$$

where $I_{corr,}$, b_a and b_c are the corrosion current density, anodic and cathodic Tafel slope, respectively. The results showed that both nanocomposite and PoPDA have R_p values higher than bare steel metal.

The obtained electrochemical corrosion parameters results of the PoPDA@MWCNTs and PoPDA@FMWCNTs nanocomposites are compared with other compounds coated steel on the basis of I_{corr} and E_{corr} found from literatures and summarized in Table 2. According to this data, the PoPDA@MWCNTs and PoPDA@FMWCNTs nanocomposites have low I_{corr} and relatively high E_{corr} in comparison with some previously reported coating based on aniline derivatives. This shows that PoPDA based nanocomposites can be a good candidate for the applications related to corrosion protection.

Table 1

Fig. 5

Table 2

Electrochemical impedance spectroscopy

The other way to evaluate the protection of the steel by the nanocomposite films that are deposited on the metal surface is by using Electrochemical Impedance Spectroscopy (EIS). The surface resistances of uncoated and coated steel in NaCl solution (3.5% w/w) were investigated using EIS technique and reported here in terms of Nyquist plots.

The Nyquist plots of uncoated steel, PoPDA, PoPDA@FMWCNTs, and PoPDA@MWCNTs nanocomposites coated steel samples after immersion in NaCl solution (3.5% w/w) is shown in Fig. 6. The shapes of the Nyquist plots for all samples show depressed semicircle in high frequency region. The diameter of depressed semicircle shows the charge transfer resistance (R_{ct}). The R_{ct} values for the PoPDA@MWCNTs nanocomposite coated steel (120 KΩ) appeared to be significantly higher than those of the PoPDA@FMWCNTs nanocomposite (74 KΩ), and PoPDA (14 KΩ) coated steel and uncoated steel (5 KΩ). The higher R_{ct} in PoPDA@MWCNTs nanocomposite coated steel is probably ascribed to the existence of MWCNTs in the nanocomposite matrix which blocks the access of the aggressive electrolyte to the reactive metal surface. Also, it seems that the lower impedance observed in PoPDA@FMWCNTs nanocomposite coated steel is due to the less hydrophobic nature of the coating. The percentage of inhibition efficiency (I.E. %) of synthesized materials coated steel was calculated as follows [30]:

$$IE\% = \frac{R_{ct}(coated) - R_{ct}(uncoated)}{R_{ct}(coated)} \qquad (2)$$

where R_{ct} (coated) and R_{ct} (uncoated) are the charge transfer resistance values with and without synthesized material coatings respectively. Results showed that the coated samples exhibited higher R_{ct} values compared to uncoated sample. Also, the percentage of corrosion inhibition efficiency for the PoPDA, PoPDA@MWCNTs and PoPDA@FMWCNTs nanocomposites coated steel is 64%, 95% and 93%, respectively. The corrosion inhibition mechanism for the PoPDA coated steel is due to the formation of an insoluble stable iron oxide-PoPDA complex at the metal/polymer interface[11]. In the PoPDA nanocomposites coated steel, probably the presence of the MWCNTs (functionalized and un-functionalized) can form an inhibiting film which protects steel against of corrosion. It seems that the mechanism of

corrosion protection by nanocomposites includes the formation of a stable interphase between the nanocomposite and steel where act as a barrier against corrosive ions, and inhibition of charge transfer from the metal surface to corrosive ion or vice versa due to the electrical conductivity of the PoPDA@MWCNTs and PoPDA@FMWCNTs nanocomposites. The Nyquist plots of uncoated steel and PVB coated steel in 3.5 w/w % NaCl solution are presented in Fig. S6 in the Supplementary data.

Fig. 6

Open circuit potential (OCP) measurements

The open circuit potential (OCP) of uncoated steel (a) and PoPDA (b), PoPDA@MWCNTs (c) and PoPDA@FMWCNTs (d) coated steel immersed in corrosive medium (NaCl solution (3.5%)) for 300 min are given in Fig. 7. The initial values measured for the bare steel, PoPDA, PoPDA@MWCNTs and PoPDA@FMWCNTs nanocomposites coated steel were -0.17 V, -0.16 V, -0.15 V and -0.04 V, respectively. All measurements were catodic potential values. After 300 min of exposure time, E_{ocp} values measured for PoPDA, PoPDA@MWCNTs and PoPDA@FMWCNTs nanocomposites were 0.06 V, 0.07 V, and 0.09 V, respectively, which are anodic with respect to that measured for uncoated steel electrode −0.11 V under the same condition. Surprisingly, the measured E_{ocp} values of PoPDA, PoPDA@MWCNTs and PoPDA@FMWCNTs nanocomposites increased. It seems the increase of the potential indicates the presence of electrostatic interaction between synthesized materials and steel surface. These results demonstrate that PoPDA, PoPDA@MWCNTs and PoPDA@FMWCNTs nanocomposites are showing barrier behavior by limiting the motion of corrosive agent toward the underlying metal and are acting as active coating affecting the

formation of the passive oxide. Also, these results displayed that E_{ocp} of PoPDA@FMWCNTs nanocomposite coated steel lower than that of PoPDA@MWCNTs nanocomposite. It can therefore be concluded that the presence of carboxylic groups in the MWCNTs is effective factor against of steel corrosion and, as a result, E_{ocp} of PoPDA@FMWCNTs nanocomposite decreased. The OCP measurements for uncoated steel and PVB coated steel in 3.5 wt % NaCl solution are shown in Fig. S7 in Supplementary data.

Fig. 7

Conclusions

The PoPDA@MWCNTs and PoPDA@FMWCNTs nanocomposites as anti-corrosion protection coating for the steel were successfully fabricated via the in situ emulsion polymerization. The presence of the MWCNTs and FMWCNTs in the nanocomposites enhanced the electrical conductivity, crystalline nature and thermal stability than that of bare PoPDA. The SEM micrographs of nanocomposites confirmed that they are fabricated successfully. Potentiodynamic polarization, EIS and OCP studies revealed that the PoPDA based nanocomposites act as a protective layer on steel against corrosion in a 3.5 wt% NaCl solution. The corrosion rate of PoPDA@MWCNTs nanocomposite coated steel is lower than that of bare steel and the I.E is found to be 95%. The higher corrosion protection ability of PoPDA@MWCNTs nanocomposite is probably due to the formation of uniform passive film on iron surface.

Acknowledgment

The research work has been supported by research grant from the University of Mazandaran.

References

1. E. N. Zare, M. M. Lakouraj, and A. Ramezani, *Adv. Polym. Technol.*, 2015, **00**, 1–11.
2. M. Baghayeri, E. N., Zare, and M.M. Lakouraj, *Microchim. Acta*, 2015, **182**, 771–779.
3. A. Olad, A. Rashidzadeh, and M. Amini, *Adv. Polym. Technol.*, 2012, **32**, 1–10.
4. Y. Haldorai, W. S. Lyoo, and J. Shim, *Colloid Polym. Sci.*, 2009, **287**, 1273–1280.
5. E. N. Zare, M. M. Lakouraj, P. N. Moghadam, and R. Azimi, *Polym. Compos.*, 2013, **34**, 732–739.
6. G. Spinks, S. Shin, G. Wallace, P. Whitten, I. Kim, and S. Kim, *Sensors Actuators B Chem.*, 2007, **121**, 616–621.
7. P. Hojati-talemi and G. P. Simon, *J. Phys. Chem. C*, 2010, **114**, 13962–13966.
8. S. Jaidev, Ramaprabhu, *Mater. Chem.*, 2012, **22**, 18775–18783.
9. Y. Peng, J. Ji, Y. Zhang, H. Wan, and D. Chen, *Enviromental Prog. Sustain. Energy*, 2013, **33**, 123–130.
10. M. M. Lakouraj, E. N. Zare, and P. N. Moghadam, *Adv. Polym. Technol.*, 2014, **33**, 21385(1–7).
11. P. Muthirulan and N. Rajendran, *Surf. Coat. Technol.*, 2012, **206**, 2072–2078.
12. P. Muthirulan, N. Kannan, and M. Meenakshisundaram, *J. Adv. Res.*, 2013, **4**, 385–392.
13. K. Balasubramanian and M. Burghard, *Small*, 2005, **1**, 180–192.
14. Z. Spitalsky, D. Tasis, K. Papagelis, and C. Galiotis, *Prog. Polym. Sci.*, 2010, **35**, 357–401.
15. N. Gopal, S. Rana, J. Whan, L. Li, and S. Hwa, *Prog. Polym. Sci.*, 2010, **35**, 837–867.
16. S. Sathiyanarayanan, S. S. Azim, and G. Venkatachari, *Synth. Met.*, 2007, **157**, 205–213.
17. A. Madhan Kumar and Z. M. Gasem, *Prog. Org. Coatings*, 2015, **78**, 387–394.

18. M. Ioni and A. Prun, *Prog. Org. Coatings*, 2011, **72**, 647–652.

19. A. Ganash, *J. Nanomater.*, 2014, **2014**, 1-8.

20. D. Lenz, M. Delamar, and C. Ferreira, *J. Electroanal. Chem.*, 2003, **540**, 35–44.

21. A. Emamgholizadeh, A. Ali, A. Omrani, and A. Rostami, *Prog. Org. Coatings*, 2015, **82**, 7–16.

22. Y. Haldorai, W. S. Lyoo, and J.-J. Shim, *Colloid Polym. Sci.*, 2009, **287**, 1273–1280.

23. H. Zhong, R. Yuan, Y. Chai, W. Li, X. Zhong, and Y. Zhang, *Talanta*, 2011, **85**, 104–111.

24. Y. Lin and T. Wu, *Compos. Sci. Technol.*, 2009, **69**, 2559–2565.

25. H. Wang, J. Li, X. Zhang, Z. Ouyang, Q. Li, Z. Su, and G. Wei, *RSC Adv.*, 2013, **3**, 9304-9310.

26. J. Qian, Q. Zhao, J. Qian, M. Zhu, and Q. An, *J. Mater. Chem.*, 2009, **19**, 8732-8740.

27. M. M. Lakouraj, G. Rahpaima, and E. N. Zare, *Chine. J. Polym. Sci*., 2014, **32**, 1489–1499.

28. P. P. Deshpande, S. S. Vathare, S. T. Vagge, E. Tomšík, J. Stejskal, *Chemical Papers*, 2013, **67**(8), 1072-1078.

29. C. H. Chang, T. C. Huang, C. W. Peng, T. C. Yeh, H. I. Lu, W. I. Hunga, C. J. Weng, T. I. Yang, J. M. Yeh, *Carbon*, 2012, **50**, 5044–5051.

30. K. Farhadi, H. Zebhi, P. N. Mogadam, and M. Eshaghi, *Synth. Met.*, 2014, **195**, 29–35.

Captions

Table 1. Electrochemical corrosion parameters of prepared coating materials

Table2. Comparison of electrochemical corrosion parameters for various samples coated steel in 3.5% NaCl solution

Scheme 1. The synthesis procedure for fabrication of PoPDA@FMWCNTs nanocomposite through emulsion polymerization technique and electrode construction pathway

Fig. 1. FTIR spectra of PoPDA@MWCNTs and PoPDA@FMWCNTs nanocomposites

Fig.2. XRD patterns of PoPDA@MWCNTs and PoPDA@FMWCNTs nanocomposites

Fig.3. SEM micrographs of PoPDA@MWCNTs (a) and PoPDA@FMWCNTs (b) nanocomposites

Fig. 4. TGA thermograms of PoPDA@MWCNTs and PoPDA@FMWCNTs nanocomposites

Fig. 5. Tafel plots for bare steel, PoPDA, PoPDA@MWCNTs, and PoPDA@FMWCNTs coated steel electrode measured in 3.5 wt. % NaCl aqueous solution

Fig. 6. Nyquist plots of bare steel, PoPDA, PoPDA@MWCNTs and PoPDA@FMWCNTs coated steel electrode measured in 3.5 wt. % NaCl aqueous solution

Fig. 7. Open circuit potential measurements for bare steel (a), PoPDA (b), PoPDA@MWCNTs (c) and PoPDA@FMWCNTs (d) coated steel electrode in 3.5 wt. % NaCl aqueous solution

Table 1: Electrochemical corrosion parameters of prepared coating materials

Samples	Bare Steel	PoPDA	PoPDA@MWCNTs	PoPDA@FMWCNTs
E_{corr} (mV)	-184	-163	-113	-153
I_{corr} (μA cm^{-2})	2.51	0.562	0.012	0.028
R_p (KΩ cm^2)	0.43	0.83	0.96	3.88

Table2. Comparison of electrochemical corrosion parameters for various samples coated steel in 3.5% NaCl solution

Sample	E_{corr} (mV)	I_{corr} (μA cm^{-2})	References
PoPDA@MWCNTs	-113	0.012	Present work
PoPDA@FMWCNTs	-153	0.028	Present work
Poly(o-phenylenediamine) nanofibers	-174	0.114	[12]
Polyaniline/FMWCNT	-505	0.034	[17]
Poly(o-phenylenediamine)/ZnO	-36	0.010	[19]
Polyaniline/ MWCNTs	-564	12.6	[28]
Polyaniline/graphene	-584	1.38	[29]
Nano-colloidal polyaniline	-505	0.034	[30]

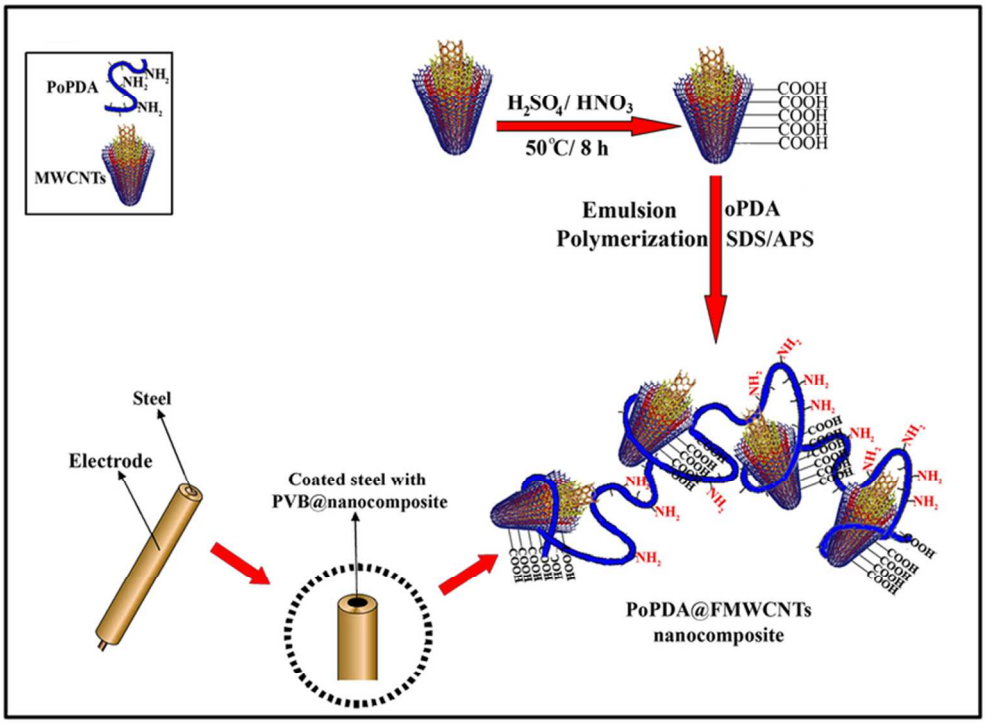

Scheme 1

The synthesis procedure for fabrication of PoPDA@FMWCNTs nanocomposite through emulsion polymerization technique and electrode construction pathway
71x55mm (300 x 300 DPI)

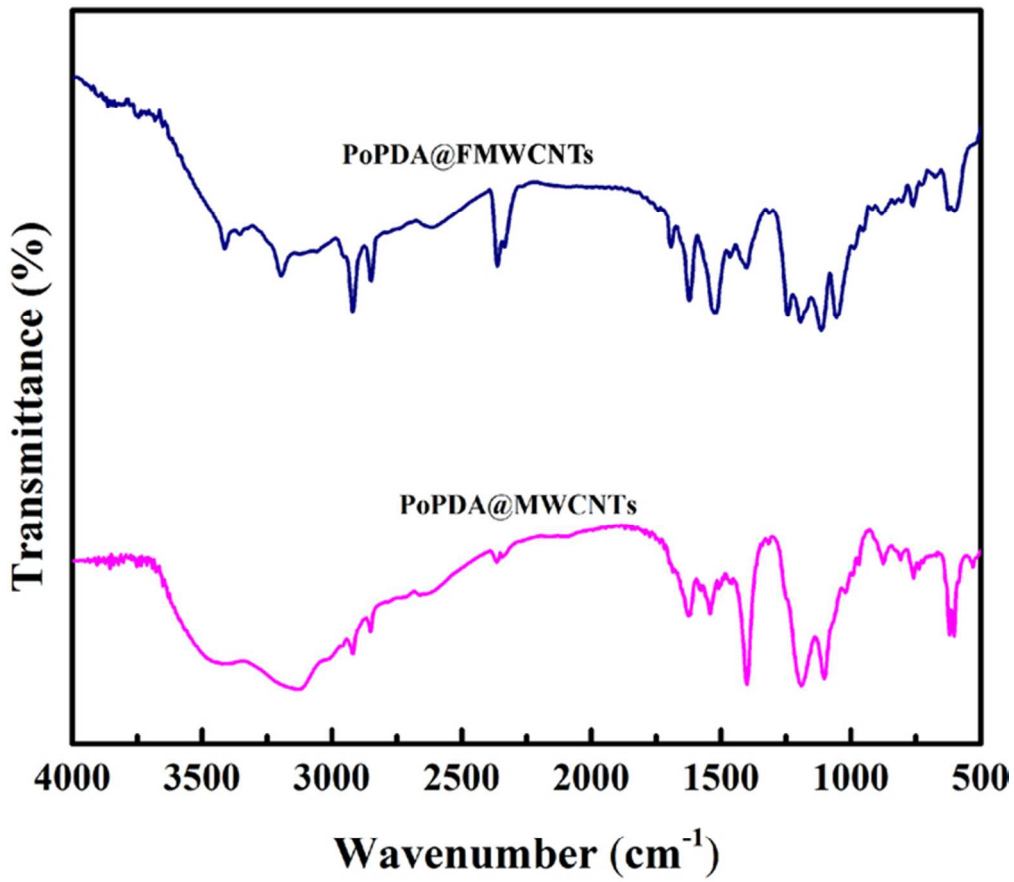

Fig 1

FTIR spectra of PoPDA@MWCNTs and PoPDA@FMWCNTs nanocomposites
59x55mm (300 x 300 DPI)

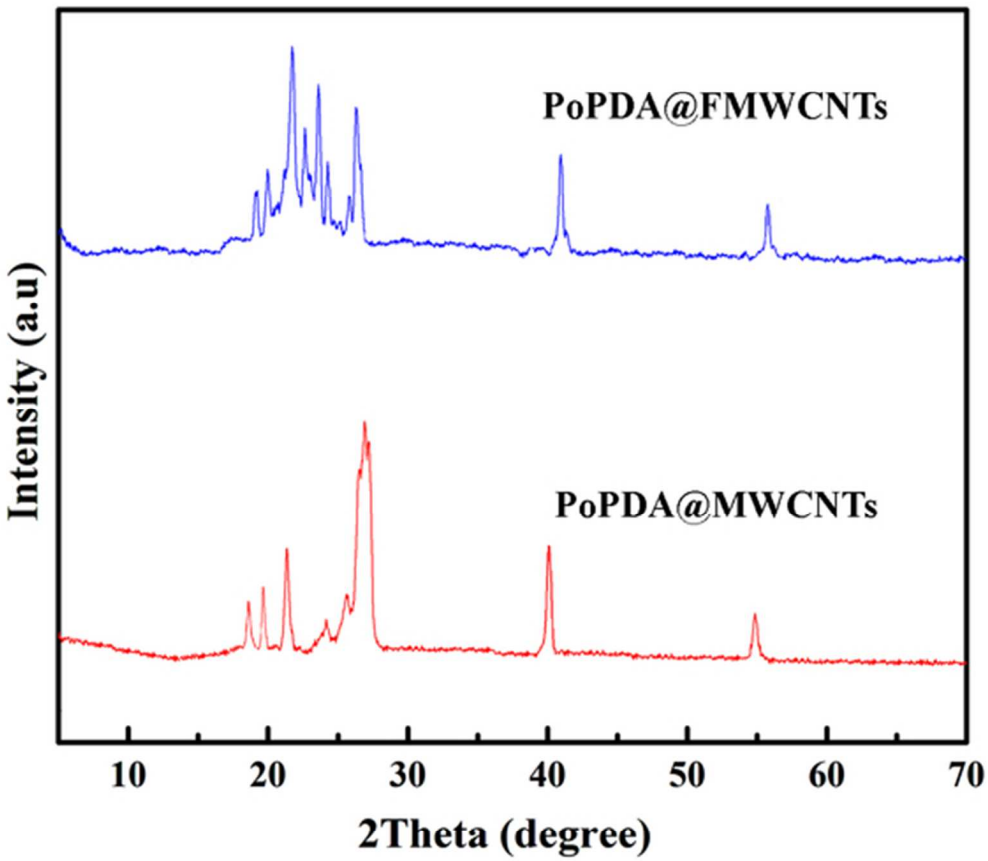

Fig 2

XRD patterns of PoPDA@MWCNTs and PoPDA@FMWCNTs nanocomposites
48x45mm (300 x 300 DPI)

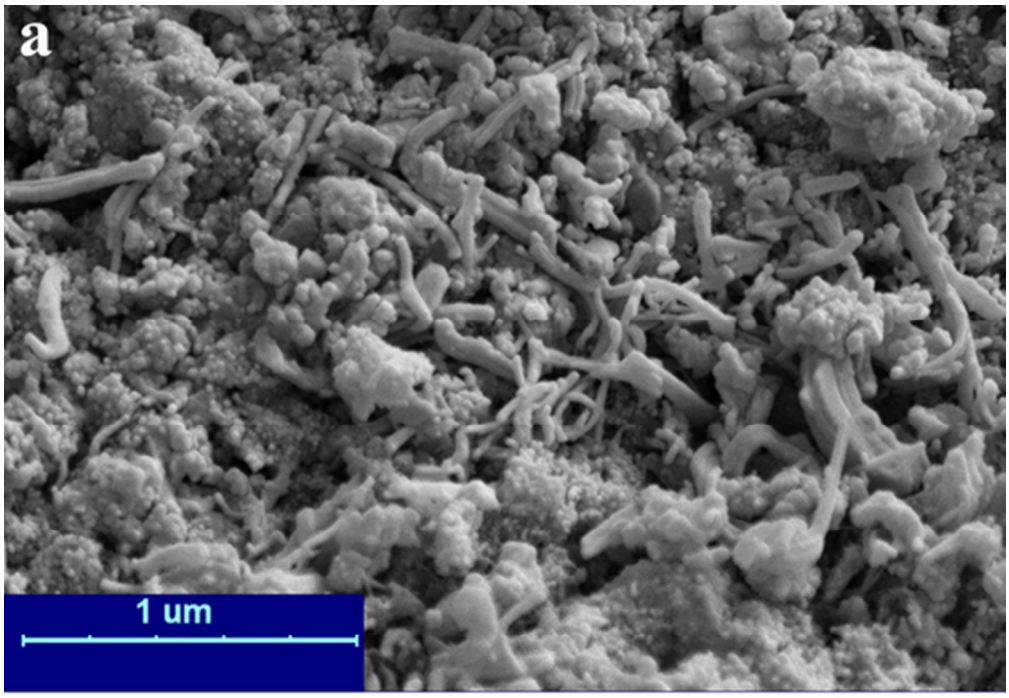

Fig. 3a

SEM micrographs of PoPDA@MWCNTs (a)
46x34mm (300 x 300 DPI)

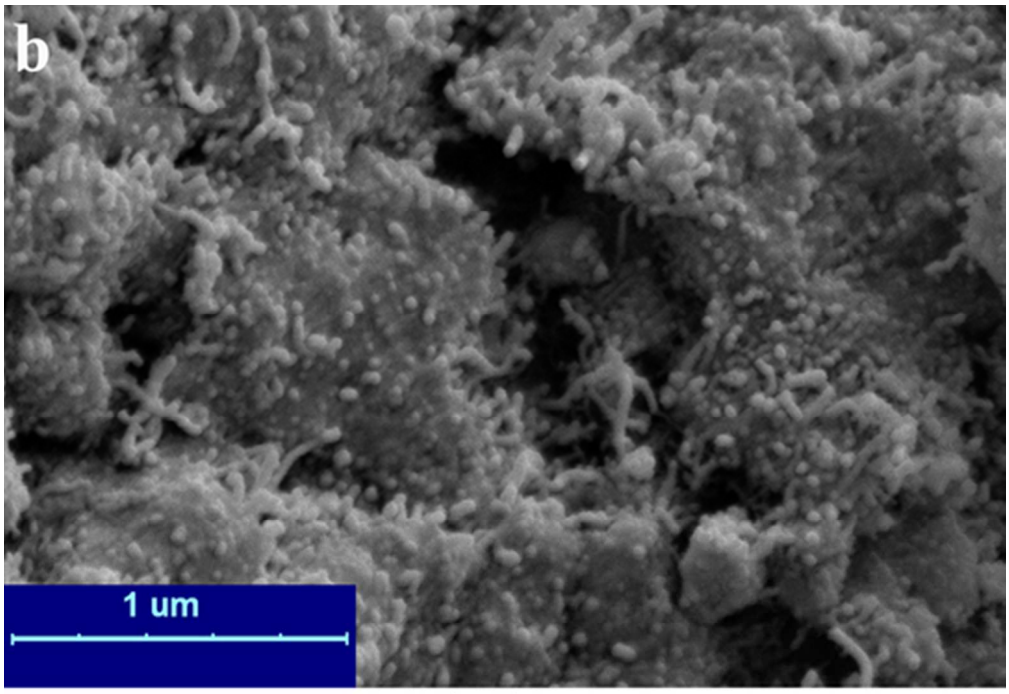

Fig. 3b

SEM micrographs of PoPDA@FMWCNTs (b) nanocomposites
45x32mm (300 x 300 DPI)

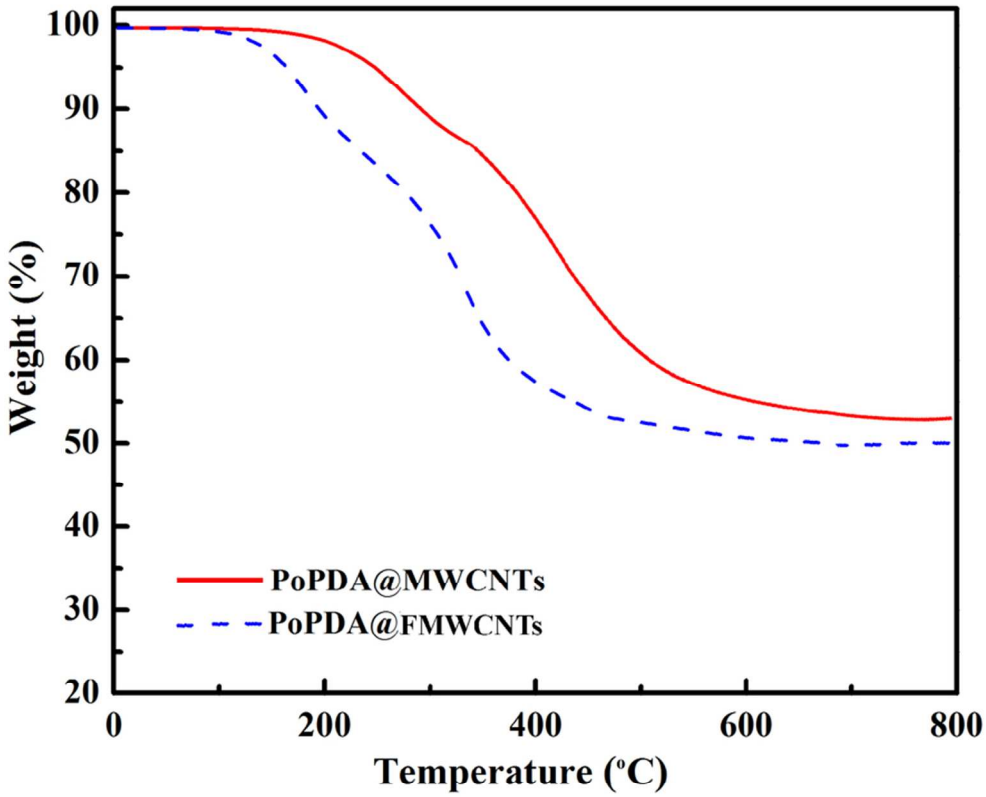

Fig 4

TGA thermograms of PoPDA@MWCNTs and PoPDA@FMWCNTs nanocomposites
75x68mm (300 x 300 DPI)

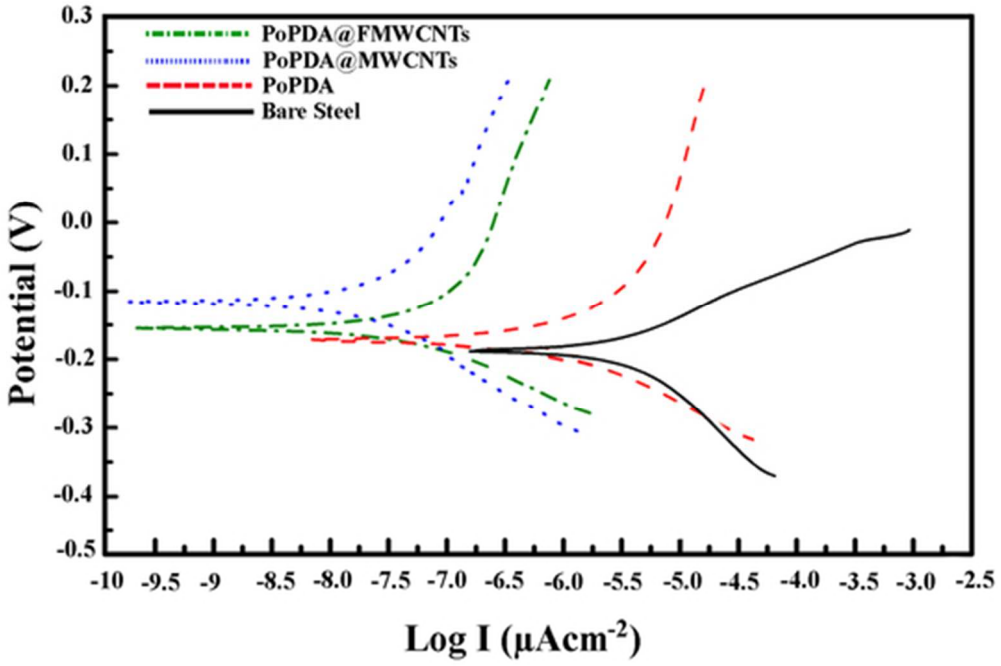

Fig. 5

Tafel plots for bare steel, PoPDA, PoPDA@MWCNTs, and PoPDA@FMWCNTs coated steel electrode measured in 3.5 wt. % NaCl aqueous solution
45x32mm (300 x 300 DPI)

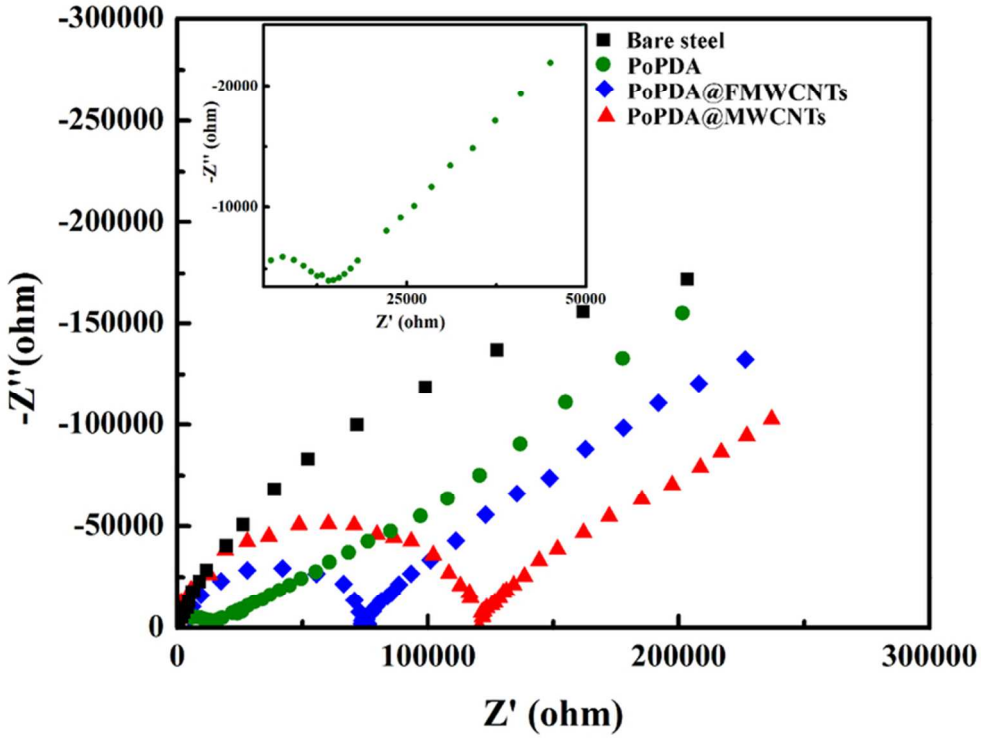

Fig. 6

Nyquist plots of bare steel, PoPDA, PoPDA@MWCNTs and PoPDA@FMWCNTs coated steel electrode measured in 3.5 wt. % NaCl aqueous solution
68x55mm (300 x 300 DPI)

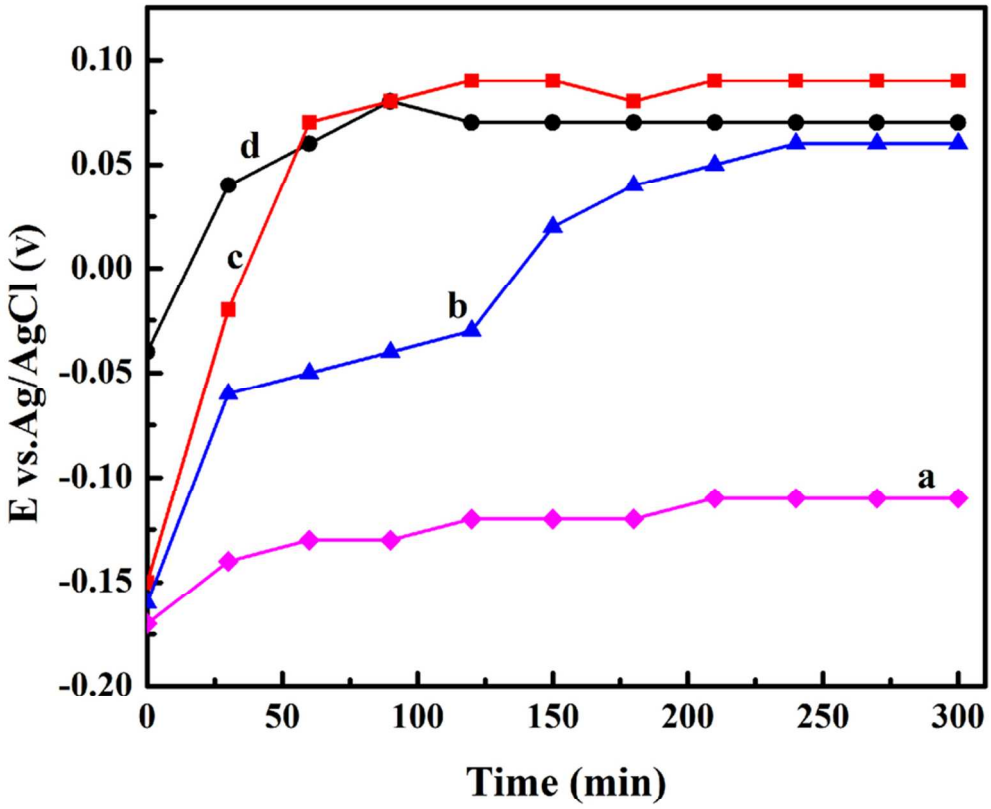

Fig 7

Open circuit potential measurements for bare steel (a), PoPDA (b), PoPDA@MWCNTs (c) and PoPDA@FMWCNTs (d) coated steel electrode in 3.5 wt. % NaCl aqueous solution
78x71mm (300 x 300 DPI)